Stresses and first-order dislocation energetics in equilibrium Stranski-Krastanow islands

B. J. Spencer
Department of Mathematics, State University of New York at Buffalo, Buffalo, New York 14260-2900

J. Tersoff
IBM Research Division, Thomas J. Watson Research Center, P.O. Box 218, Yorktown Heights, New York 10598

(Received 15 September 2000; published 7 May 2001)

We numerically determine the state of stress in two-dimensional Stranski-Krastanow islands having equilibrium shape. These calculations reveal important generic characteristics and quantitative details of the stress state in equilibrium islands, including stress relaxation and stress concentration. We also use the stresses to determine the first-order energy of introducing dislocations of different Burgers vectors into Stranski-Krastanow islands. These results characterize the ''energy wells'' sought by dislocations to relieve the misfit stress, and suggest that misfit dislocations in islands segregate according to the orientation of their Burgers vector. This segregation allows for more efficient relief of the nonuniform strain in misfitting islands.

DOI: 10.1103/PhysRevB.63.205424 PACS number(s): 68.55.Jk, 81.10.Aj

I. INTRODUCTION

For a number of years there has been much interest in the ''island'' growth mode of strained solid films, first as a degradation mechanism during planar film growth, and more recently as a means to manufacture quantum dot arrays for electronics applications.[1,2] It is generally understood that islands form to reduce the total elastic strain energy in these systems and are a manifestation of a stress-driven morphological instability of planar layers.[3–14] In recent years much progress has been made in understanding the characteristics of island formation,[15–35] but much of this theoretical work has been based on *assumed* simple geometries for the island shape. These shapes include the arc of a circle,[29] a cone,[23] full or truncated pyramids,[16,34,28] and rectangles.[22] While these assumed-shape calculations give valuable information about how the properties of the island vary as the geometry is varied, they do not allow for the island to assume the *actual shape* that minimizes the energy. In contrast to the large number of assumed-shape calculations, there are only a few papers that have solved the free boundary problem for the island shape.[21,26,30,31,36] All of these calculations, like those presented here, have been for two-dimensional, isotropic systems, corresponding to island ''ridges'' in three dimensions. Both Chiu and Gao[21] and Kukta and Freund[30] used boundary layer models to account for the wetting of the substrate by the film and determine island shapes and characteristics for small to moderate size islands. In Ref. 26 we presented an asymptotic theory for small islands, which shows that the island has a minimum width, while in Ref. 31 we presented results describing the shape of islands as the volume is increased from zero to large values.

In this paper, we detail the stress distribution accompanying the equilibrium shape of an island. We also use the stresses in a simple calculation to determine the energy of introducing a dislocation into the island based on a first-order expansion of the energy in the Burgers vector. These results suggest a segregation mechanism for dislocations in Stranski-Krastanow islands: the Burgers vector of a dislocation near the island edge has a preferred orientation that relieves the misfit strain *and* the bending of the film/substrate interface induced by the misfitting island.[36]

The rest of the paper is organized as follows. In Sec. II we describe the calculation of the equilibrium shape and stresses. In Sec. III we present the results for the stresses in islands of different sizes. In Sec. IV we describe a simple calculation of the first-order energy of a dislocation and discuss the results. Finally, in Sec. V we summarize our main findings.

II. EQUILIBRIUM MODEL

We consider a single-component, two-dimensional, fully isotropic, epitaxially strained system with the film/substrate interface given by $z=0$ and the film surface described by $z=h(x)$ with $h(x)>0$. The islands we describe in two dimensions are equivalent to elongated island ''ridges'' in three dimensions. The details of the model are the same as presented in Refs. 31 and 36.

A difference in lattice parameters between the film and substrate generates a misfit strain in the film. We take the film and substrate to be linearly elastic materials and assume that the film and substrate have identical elastic constants. The elasticity problem for the film/substrate system is therefore equivalent to that for a stressed, semi-infinite solid [since $h(x)>0$]. The stress $\mathbf{T}$ satisfies $\nabla\cdot\mathbf{T}=0$, with the boundary conditions $\mathbf{n}\cdot\mathbf{T}=0$ on $z=h(x)$, and $\mathbf{T}\rightarrow\mathbf{T}_0$ as $z\rightarrow-\infty$. Here $\mathbf{T}_0$ is the uniaxial (misfit) stress for a uniform film, and $\mathbf{n}$ is the unit normal to the film surface. The stresses in the film are then given by $\boldsymbol{\sigma}=\mathbf{T}$, and the stresses in the substrate are given by $\boldsymbol{\sigma}=\mathbf{T}-\mathbf{T}_0$.

We assume that mass transport occurs solely by surface diffusion in response to gradients in a chemical potential μ. Equilibrium morphologies thus correspond to a constant chemical potential along the film surface. The chemical potential has two contributions, $\mu=\gamma\kappa+S$ (see, for example, Ref. 3). Here γ is the surface energy of the film, κ is the curvature of the film surface, and S is the strain energy density, $S=\frac{1}{2}\mathrm{Tr}(\mathbf{TE})$, where $\mathbf{E}$ is the strain tensor.

The systems studied to date are primarily those for which the film wets the substrate, leading to islands surrounded by a thin wetting layer (the Stranski-Krastanow growth mode).

The presence of the wetting layer in effect dictates the contact angle at the island edge. To account for the energetics of the wetting layer, we employ the ''glued wetting layer model.''[26] As shown in Ref. 37, this model can be derived from transition layer models[21,30] for the material properties across the interface between the film and substrate, and represents the limiting case of an abrupt change in the material properties at the film/substrate interface. With this model, the Stranski-Krastanow island morphology is described by

$$\mu = \gamma\kappa + S \quad \text{for } h(x) > 0 \quad \text{(on the island)},$$

$$h'(x) = 0 \quad \text{at the island edge},$$

$$h(x) = 0 \quad \text{otherwise (on the wetting layer)}. \tag{1}$$

This set of equations for the film morphology corresponds to constant chemical potential μ everywhere on the surface of the film and the thin wetting layer.

The strained film has a characteristic strain energy density $S_0 = \frac{1}{2}\mathrm{Tr}(\mathbf{T}_0\mathbf{E}_0)$, where $\mathbf{T}_0$ and $\mathbf{E}_0$ are the stress and strain tensors for a uniform film. The equilibrium island shape represents a balance between surface energy and strain energy terms. As a result, it has a characteristic length $l = \gamma/S_0$. In the results that follow, we scale all lengths by l, all energy densities by S_0, and all stresses by the misfit stress T_0.

The elasticity problem for the island is solved numerically using the boundary integral method developed in Ref. 38. In this formulation, the components of the stress tensor $\mathbf{T}$ are represented in terms of the complex variable $\zeta = x + iz$, where

$$T_{xx} + T_{zz} = 4\,\mathrm{Re}[\phi'(\zeta)] \tag{2}$$

and

$$T_{zz} - T_{xx} + 2iT_{xz} = 2[\zeta^*\phi''(\zeta) + \psi'(\zeta)], \tag{3}$$

where ζ^* is the complex conjugate of ζ, and $\phi(\zeta)$ and $\psi(\zeta)$ are complex valued functions that are analytic in the film and substrate. For a given island shape the solution to the boundary integral equation provides the boundary values of $\phi(\zeta)$ and $\psi(\zeta)$ along the film surface. The derivatives of these functions are then evaluated numerically along the boundary, and the interior values of $\phi(\zeta)$, $\psi(\zeta)$, and their derivatives are determined by analytic continuation using Cauchy integrals of the boundary values. The individual components of the stresses are determined by taking the appropriate combinations of the real and imaginary parts of Eqs. (2) and (3). To determine the equilibrium island shape $z = h(x)$, the stress computations are used in an iterative numerical method to determine the island shape that satisfies the free boundary equation (1).

The details of the island shape are presented in Ref. 31. There is a family of island shapes parametrized by the (dimensionless) island volume per unit length V. The main features of these results are that small islands have a fixed width and vanishing thickness; the height/width aspect ratio increases as the island size increases; and large islands tend toward a ''ball'' shape. Here we present the details and consequences of the stress fields associated with these equilibrium island morphologies.

III. STRESSES IN EQUILIBRIUM ISLANDS

Figures 1(a)–1(i) show the components of the stress within the island and substrate for islands of increasing volume ($V = 0.1,1,10$). From the figure, a number of general observations about the stresses can be made.

(1) *Relaxation of the misfit stress at the island peak.* As the island volume increases, the misfit stress σ_{xx} at the top of the island is relaxed from that of the uniform film ($\sigma_{xx} = 1$) toward $\sigma_{xx} = 0$. (The stress actually over-relaxes by a small amount for large enough V and then approaches complete relaxation for larger islands.[31])

(2) *Stress in the substrate directly under the island.* Relaxation of the island occurs in part by deformation of the substrate, causing a stress in the substrate of the opposite sign to the island mismatch stress. As the island volume increases, the substrate stress increases. At small island volumes this effect is the sole mechanism for relaxation in the island. For large islands, this effect also contributes to strain relief, but the bulk of the relaxation is due to the relaxation at the free surface of the island.

(3) *Stress concentration in the island and substrate near the island edge.* As the island volume increases, there is a sharpening and strengthening of the stress concentration near the island edge. The stress concentration is not focused at the island edge itself, but is on the island surface a small distance away from the island edge. For a nonzero contact angle there would be a stress singularity at the corner.[39] Since the contact angle for the Stranski-Krastanow island is zero, there is no singularity and maximum stress does not lie at the island edge. However, the ''effective'' contact angle (as measured a small distance away from the edge[31]) increases with V and causes the increasing stress near the edge. Figures 1(j)–1(l) show an expanded view of the misfit stress concentration near the right edge of the island for $V = 0.1$, $V = 1$, and $V = 10$.

(4) *Decay of the stresses vertically in the substrate.* Figure 1 shows that the stresses in the substrate induced by the island morphology become small relative to T_0 within about one island height of the substrate surface.

(5) *Decay of the stresses laterally away from the island.* Figure 1 shows that the stresses at the substrate surface become small relative to T_0 within less than one island height of the island edge.

Overall, in small islands the state of stress is characterized by nearly uniform misfit in the island with very little stress in the substrate. The small amount of relaxation that does occur is primarily due to the accommodation of part of the mismatch by the underlying substrate, leading to an island with nearly uniform σ_{xx} and small σ_{xz}. As the island volume increases, more of the island becomes relaxed, but there is a sharp focusing of the stress concentrations near the island edge, which include relatively large dilatational and shear stresses. In addition, on either side of the island/substrate interface underneath the center of the island are regions that remain stressed (with opposite sign) as the island volume increases.

The implication of the short-range lateral decay of the elastic fields is that any elastic interaction between neighbor-

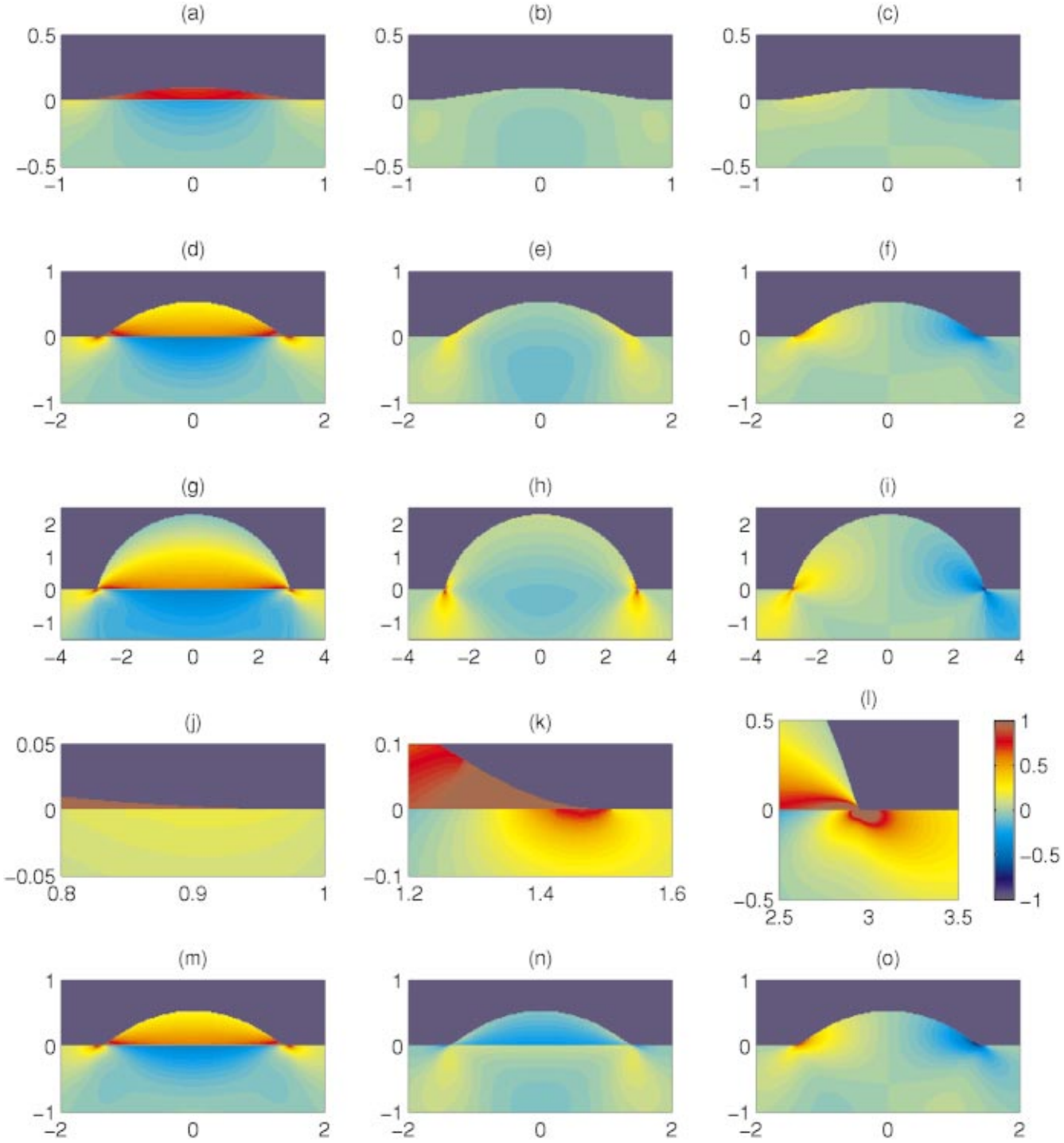

FIG. 1. (Color) Stresses and strains of equilibrium islands. All stresses and strains are scaled relative to the misfit stress and strain for a planar film. Stresses in a small island ($V=0.1$): (a) σ_{xx}, (b) σ_{zz}, (c) σ_{xz}. Stresses in a medium sized island ($V=1$): (d) σ_{xx}, (e) σ_{zz}, (f) σ_{xz}. Stresses in a large island ($V=10$): (g) σ_{xx}, (h) σ_{zz}, (i) σ_{xz}. Stress σ_{xx} near the island edge: (j) $V=0.1$, (k) $V=1$, (l) $V=10$. Strains in a medium sized island ($V=1$): (m) E_{xx}, (n) E_{zz}, (o) E_{xz}.

ing islands farther apart than their height is likely to be weak relative to the energies determining their shape. Consequently, the island shape should be relatively insensitive to the island separation until the distance between neighboring islands is smaller than the island height. These results are consistent with the recent experiments of Floro *et al.*[40] In their experiments, SiGe films were grown on Si substrates and the island shapes were monitored as the film was deposited. During the initial stages of deposition, the islands were small and well separated. During the later stages the islands became larger and began to impinge on one another. It was found that the elastic interaction due to this impingement resulted in a morphology change in the island from ''huts'' to ''domes.'' While the details of the morphologies (huts in

particular) are strongly influenced by the anisotropy in the surface energy, which we do not take into account in our theory, the qualitative feature of a shape transition is consistent with the short-range decay of the stress fields. Because of the rapid decay, the shape transition due to the elastic interaction of neighboring islands occurs only when the islands start to impinge.

While the above results focus on the stresses, the associated strains can be determined from the stresses using the constitutive laws for isotropic linear elasticity. Figures 1(m)–1(o) show the strains in the film and the substrate for a moderate size island, $V=1$ (with Poisson ratio $\nu=0.25$). As expected, the strains mimic the stresses with slight differences due to the Poisson effect, primarily in the E_{zz} component of the strain due to the necessary vertical compression/stretching of the film to accommodate the tensile/compressive misfit in the lateral directions.

IV. FIRST-ORDER ENERGY OF INTRODUCING A DISLOCATION

The stress distribution in the island and substrate can be used to give a first-order estimate of the energy required to introduce a dislocation into the system. In general, the total energy of introducing a dislocation into the island consists of a term that is linear in the Burgers vector $\boldsymbol{b}$ and terms that are higher order in $\boldsymbol{b}$. While including the higher-order terms is essential to understanding when it is energetically favorable to introduce a dislocation, such calculations require solving the elasticity problem in the presence of the dislocation. While these calculations have been carried out for the case of islands of prescribed shape,[29] such calculations have not been attempted with the free boundary problem for the actual equilibrium island shape. In the absence of a complete treatment that includes these second-order contributions, we present here the contribution of the first-order term which gives valuable generic information about the magnitude and distribution of energy available to overcome the nucleation barrier for dislocations. In particular, we determine the variation of this first-order energy everywhere in the island and substrate to give an energy map for dislocations of different types.

The first-order energy of a dislocation is due to the force on the dislocation from the stress in the island and substrate. A dislocation line extending in the $\boldsymbol{d}$ direction with Burgers vector $\boldsymbol{b}$ experiences a Peach-Koeler force per unit length[43]

$$\boldsymbol{F}=\boldsymbol{b}\cdot\boldsymbol{\sigma}\times\boldsymbol{d}, \tag{4}$$

which is linear in the stress $\boldsymbol{\sigma}$ and the Burgers vector $\boldsymbol{b}$. Consider a dislocation line that extends perpendicular to the cross section of the two-dimensional island (directed along the ridge) with $\boldsymbol{d}=(0,1,0)$. Let the Burgers vector be $\boldsymbol{b}=b(b_x,b_y,b_z)$ where b is the length of $\boldsymbol{b}$ and (b_x,b_y,b_z) is a unit vector describing the orientation of $\boldsymbol{b}$. If this dislocation is placed on the surface of the film at point $\boldsymbol{s}$, the energy per unit length required to move the dislocation line against the Peach-Koeler force to any point $\boldsymbol{x}=(x,z)$ inside the film or substrate is

$$E(\boldsymbol{x})=-\int_{\boldsymbol{s}}^{\boldsymbol{x}}\boldsymbol{F}\cdot\boldsymbol{dp}, \tag{5}$$

where $\boldsymbol{p}$ is the path from surface point $\boldsymbol{s}$ to interior point $\boldsymbol{x}$. It is straightforward to show that the integral is path independent if $\boldsymbol{\sigma}$ corresponds to mechanical equilibrium. Thus, a consequence of the path independence is that the surface of the film corresponds to a zero energy surface, $E=0$. Therefore, the energy per unit length of introducing a dislocation at the surface and moving it to an arbitrary point $\boldsymbol{x}$ can be evaluated from a vertical path from a point on the surface $\boldsymbol{s}=(x,h(x))$ to the interior point $\boldsymbol{x}=(x,z)$ as

$$E(x,z)=b\left[b_x\int_z^{h(x)}\sigma_{xx}\,dz+b_z\int_z^{h(x)}\sigma_{xz}\,dz\right]. \tag{6}$$

Since the energy is linear in b and the stress, we can write the energy in nondimensional form as

$$\tilde{E}=\frac{E}{lbT_0}, \tag{7}$$

where T_0 is the misfit stress for a planar film and l is the length scale introduced earlier. We shall assume without loss of generality that T_0 is positive (tensile misfit) so that E and $\tilde{E}$ are of the same sign. The results for T_0 negative (compressive misfit) correspond to E of the opposite sign to $\tilde{E}$. We use our stress calculations to evaluate the integrals in Eq. (6) and determine the energy $\tilde{E}$ of moving a dislocation from the surface to any point in the interior. These results are shown in Figs. 2(a)–2(c) for $\boldsymbol{b}$ in the direction of each of the three coordinate axes.

In Fig. 2(a) the Burgers vector $\boldsymbol{b}=b(1,0,0)$ corresponds to an extra plane of atoms extending vertically downward below the dislocation. From Eq. (6) the energy is due exclusively to the σ_{xx} component of the stress. Consider the stress distribution shown in Fig. 1(d). For a tensile misfit, the tensile stress in the island tends to push this dislocation up toward the surface of the island. On the other hand, the compressive stress below the substrate tends to pull the dislocation down into the substrate. Thus, moving a dislocation from the top of the island down into the center of the island requires an increasing amount of energy to overcome the Peach-Koeler force. This energy reaches a maximum at the island/substrate interface, where the discontinuous change in the stress from tensile to compressive means that moving the dislocation further down into the substrate actually lowers the energy. Far below the island the net energy expended is zero, as it must be by virtue of the path independence of the integral and the decay of the stresses away from the island. The energy required to overcome the adverse stress field in the island generates a high-energy ''hot spot'' for the dislocation centered below the peak of the island and extending along the film/substrate interface.

Reversing the direction of the Burgers vector to $\boldsymbol{b}=b(-1,0,0)$ results in changing the sign of the energy in Fig. 2(a). Thus, $\boldsymbol{b}=b(-1,0,0)$ would have an energy ''well'' that lies below the center of the island along the island/substrate interface. Similarly, changing the sign of the

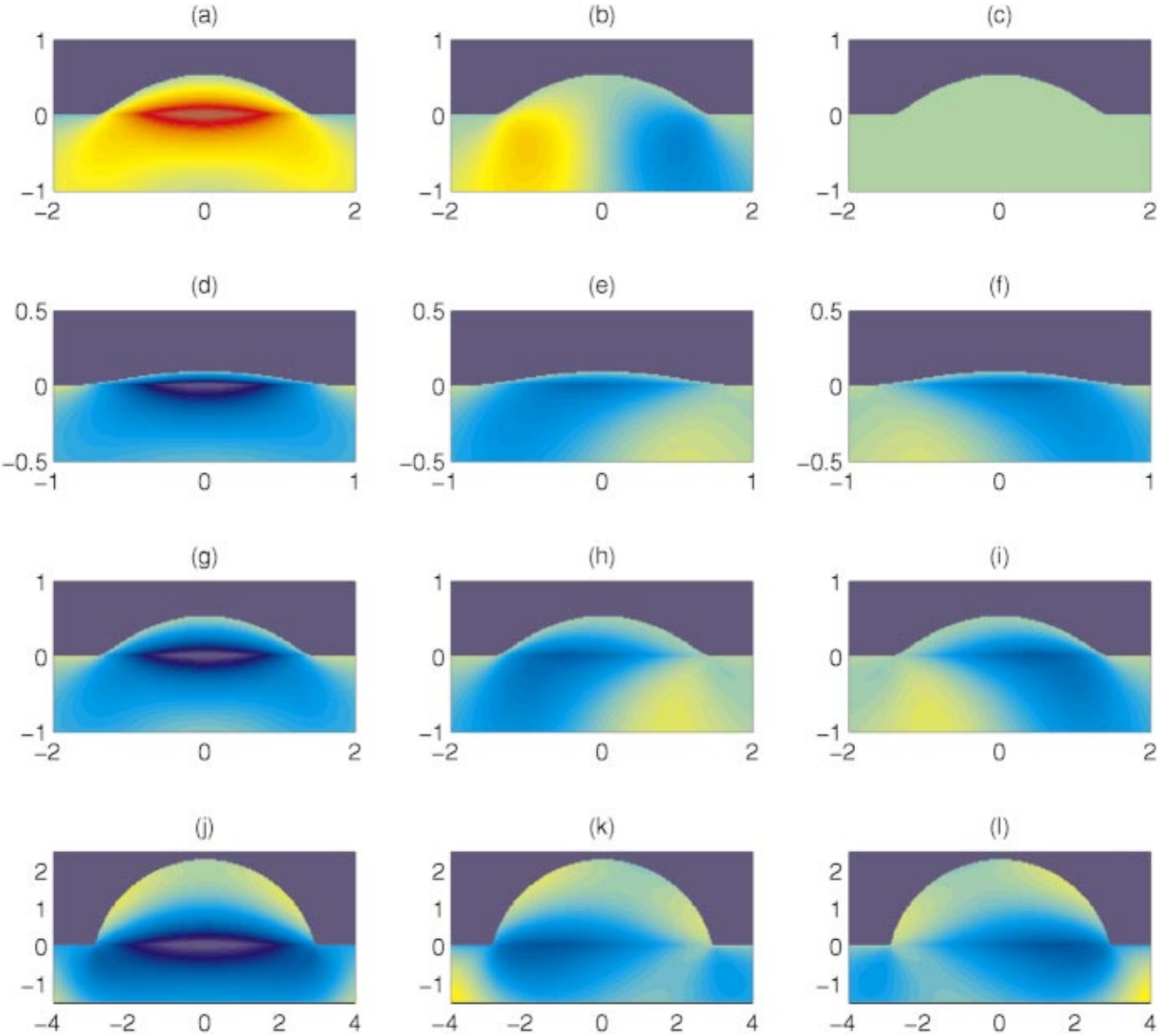

FIG. 2. (Color) First-order energy of a dislocation. All calculations are for the dislocation line $\boldsymbol{d}=(0,1,0)$ extending perpendicular to the plane of the figure. The different plots correspond to different $\boldsymbol{b}$ for different size islands. The energy for dislocations in the three coordinate directions for a medium size island ($V=1$) is shown in (a) $\boldsymbol{b}=b(1,0,0)$, (b) $\boldsymbol{b}=b(0,0,1)$, (c) $\boldsymbol{b}=b(0,1,0)$. The energetics of the three fundamental dislocation types listed in Table I are shown in (d)–(l). The island sizes are $V=0.1$ for (d)–(f); $V=1$ for (g)–(i); $V=10$ for (j)–(l). The dislocation types correspond to an edge dislocation with $\boldsymbol{b}=b(-1,0,0)$ in (d), (g), and (j); 60° dislocation with $\boldsymbol{b}=b(-1/2, \pm 1/2, -1/\sqrt{2})$ in (e), (h), and (k); and 60° dislocation with $\boldsymbol{b}=b(-1/2, \pm 1/2, +1/\sqrt{2})$ in (f), (i), and (l). The energy scale follows the same color scheme employed in Fig. 1 with maximum values $\tilde{E}=0.0655$ for $V=0.1$, $\tilde{E}=0.2111$ for $V=1$, and $\tilde{E}=0.5769$ for $V=10$.

misfit would result in a reversal of the signs of the energy. Thus, for a compressive misfit, the $\boldsymbol{b}=(1,0,0)$ dislocation (corresponding to the extra plane of atoms extending downward) has the energy minimum underneath the island while $\boldsymbol{b}=(-1,0,0)$ has the energy maximum. Similar transformations can be made for all the dislocation types discussed below.

In Fig. 2(b) the Burgers vector $\boldsymbol{b}=b(0,0,1)$ corresponds to an extra plane of atoms to the right of the dislocation line. From Eq. (6) the energy is due exclusively to the σ_{xz} component of the stress. Figure 1(f) shows the antisymmetry of the shear stress, which results in an antisymmetry of the energy. Since a negative shear stress tends to pull the dislocation line downward, there is a low-energy ''cold spot'' underneath the right edge of the island that experiences the negative shear stress. The corresponding high-energy region lies under the left edge of the island. As in case (a), reversing the sign of $\boldsymbol{b}$ results in reversing the sign of the energy in Fig. 2(b).

In Fig. 2(c) the Burgers vector $\boldsymbol{b}=b(0,1,0)$ points along the line of the dislocation. It is therefore a pure screw dislocation and does not contribute to the relaxation of the misfit stress. This is evidenced by the independence of E with respect to b_y, giving $E=0$ everywhere.

TABLE I. Summary of Burgers vectors for misfit dislocations aligned with ridge. For each of the 12 possible $\langle 110 \rangle$ crystal directions for $\boldsymbol{b}$, the corresponding (x,y,z) coordinates of $\boldsymbol{b}$ are obtained from the appropriate coordinate transformation. The column labeled ''Energy'' indicates how the first-order energy surface is related to Fig. 2.

$\boldsymbol{b}$ (crystal)	b_x	b_y	b_z	Type	Energy
$[\bar{1}10]$	-1	0	0	pure edge	Figs. 2(d,g,j)
$[1\bar{1}0]$	$+1$	0	0	pure edge	reverse sign of Figs. 2(d,g,j)
$[\bar{1}0\bar{1}],[01\bar{1}]$	$-1/2$	$\pm 1/2$	$-1/\sqrt{2}$	60° misfit	Figs. 2(e,h,k)
$[10\bar{1}],[0\bar{1}\bar{1}]$	$+1/2$	$\pm 1/2$	$-1/\sqrt{2}$	60° misfit	reverse sign of Figs. 2(e,h,k)
$[\bar{1}01],[011]$	$-1/2$	$\pm 1/2$	$+1/\sqrt{2}$	60° misfit	Fig. 2(f,i,l)
$[101],[0\bar{1}1]$	$+1/2$	$\pm 1/2$	$+1/\sqrt{2}$	60° misfit	reverse sign of Figs. 2(f,i,l)
$[110],[\bar{1}\bar{1}0]$	0	± 1	0	pure screw	$\tilde{E}=0$

The preceding results are for Burgers vectors in the direction of one of the three coordinate axes. The first-order energetics of any $\boldsymbol{b}=b(b_x,b_y,b_z)$ can be determined from the appropriate linear combination of these energies. While it is clear that the pure edge dislocation $\boldsymbol{b}=b(-1,0,0)$ has the deepest energy minimum of all possible combinations, energetics is not the sole factor that determines which dislocation type is most important for relieving the misfit strain. Another consideration is the glide plane of the dislocations. For planar (001) films with diamond cubic crystal structure, 60° misfit dislocations, which can glide at an angle to the film/substrate interface, can be more important for relieving strain (see Ref. 41 and cited references). Misfit dislocations have also been documented in nonplanar morphologies such as ridges[20] and three-dimensional islands.[42] The energetics of misfit dislocations in our two-dimensional islands can be determined by the appropriate combination of the energies from the three components of $\boldsymbol{b}$.

Consider a fcc-based crystal with a [001] substrate surface orientation. Misfit dislocations parallel to the substrate surface will then extend along the [110] and $[1\bar{1}0]$ directions. We take the island ridge to run parallel to the [110] direction and consider the energetics of $\boldsymbol{d}=[110]$ dislocations that extend parallel to the ridge. The Burgers vector for the misfit dislocation must then lie in one of the 12 possible $\langle 110 \rangle$ directions. By using the appropriate transformation of the crystal orientation to the (x,y,z) Cartesian coordinates used in the stress calculation, we obtain the equivalent $\boldsymbol{b}$ values for each of the 12 misfit dislocations. These results are summarized in Table I.

Table I shows that the 12 possible $\boldsymbol{b}$ correspond to three nontrivial energy surfaces and their reverses. We plot these three fundamental energy surfaces for a small ($V=0.1$), medium ($V=1$), and large island ($V=10$) in Figs. 2(d)–2(l).

From Fig. 2 the following observations can be made regarding the first-order energy.

(1) The pure edge b_x dislocation has a lens-shaped minimum/maximum that extends along the island/substrate interface beneath the center of the island.

(2) The pure edge b_y dislocation has an antisymmetric maximum/minimum that lies slightly inside the island edge but well into the substrate.

(3) The energy minimum for the b_x dislocation is always deeper than the b_y dislocation (and thus deeper than any mixed dislocation with the same magnitude Burgers vector).

(4) The relative size and position of the ''energy well'' structures appear to be insensitive to the change in shape associated with varying island size.

(5) 60° misfit dislocations have an off-centered energy minimum which extends below one-half of the island and lies along the island/substrate interface.

The implication of the asymmetrical energy minimum for 60° misfit dislocations means that dislocations of one orientation are preferred on one side of the island while dislocations of another orientation are preferred on the other side. On the basis of this first-order energy calculation, the asymmetry in the energies suggests that misfit dislocations in Stranski-Krastanow islands tend to segregate to one side or the other by type.

While energetics alone is not sufficient to determine the distribution of dislocations, from examining two limiting cases we confirm that the influence of the energetics on the kinetics of dislocation introduction is such that the kinetically determined distribution of dislocations will exhibit a (partial) lateral segregation by Burgers vector consistent with that suggested by the energetics.

In the limit of small driving force, when the island is barely large enough to support a dislocation, the asymmetric energetics means that the energy cost associated with the higher-order terms will be exceeded only on the energetically favored side of the island, and thus dislocations will be introduced only on that side. This scenario is most relevant when there are ample threading dislocations already in the substrate. Then, for reasonable glide mobilities, the distribution of dislocations would reflect the energetics. For islands slightly above the critical size the different orientations would have very different driving forces, leading to strong segregation.[44]

The other limit for the kinetics is that of large driving force. If there are no preexisting dislocations and the island is much larger than the critical size for dislocation introduction, then the distribution of dislocations will be controlled by the kinetics of dislocation formation. If dislocations nucleate as half loops at the island surface, then the nucle-

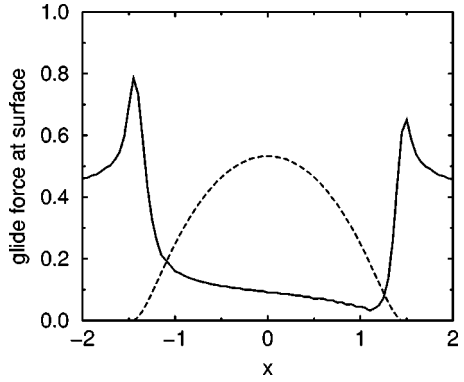

FIG. 3. Glide component of force on 60° misfit dislocation along the surface of the island. Glide force, solid line; island shape, dashed line. Energy map for dislocation is Fig. 2(h).

ation barrier depends primarily on the force on the dislocation in the glide direction at the surface. We determine this force from our calculations for the 60° misfit dislocation and island volume $V=1$. The results, Fig. 3, show a larger glide force on the side of the island with the more favorable energetics. Since the distribution is controlled by the nucleation rate, and so depends exponentially on the barrier, a small difference in first-order energetics can lead to a large degree of segregation (see, for example, Refs. 44 and 45).

Physically, the position preference of dislocations of different orientations is consistent with the efficient relief of the strain in the island. Consider an island with a compressive misfit. If the island had uniform strain then the atoms of the film would be compressed laterally and extended vertically due to the Poisson effect, as shown in Fig. 4(a). A uniform strain does not correspond to elastic equilibrium, however, and the island relaxes to a state of nonuniform strain. By integrating the strains in our calculation we determine the lattice deformations in the island after relaxation, shown in Fig. 4(b). (See Ref. 29 for the deformation accompanying a circular arc island with a compressive misfit.) The island relaxes primarily through the atoms along its surface relaxing to their original unstrained configuration. This surface relaxation is inhibited within the center of the island, as well as at the edges of the island due to contact with the substrate surface. As the island relaxes, it pushes outward from its center, pushing downward on the underlying substrate near the island edges and causing a significant ''bulging'' or bending of the film/substrate interface underneath the island.

As illustrated by Fig. 2, the strain energy of the system can be reduced by introducing the appropriate misfit dislocation at an energy well. In particular, Fig. 2(k) indicates that (reversing the sign of the energy twice) for compressive misfit the optimal location for a 60° misfit dislocation with $\boldsymbol{b}=(+1/2,\pm 1/2,-1/\sqrt{2})$ is along the film/substrate interface under the left side of the island. Similarly, the energy in Fig. 2(l) shows that for compressive misfit the optimal location for a 60° misfit dislocation with $\boldsymbol{b}=(+1/2,\pm 1/2,+1/\sqrt{2})$ is along the film/substrate interface under the right side of the island. The dislocation with an energy minimum underneath the right side of the island has a Burgers vector that corresponds to an ''extra plane of atoms'' which extends down and to the left of the dislocation. Similarly, the dislocation that is favored on the left side has the extra plane of atoms pointing down and to the right.

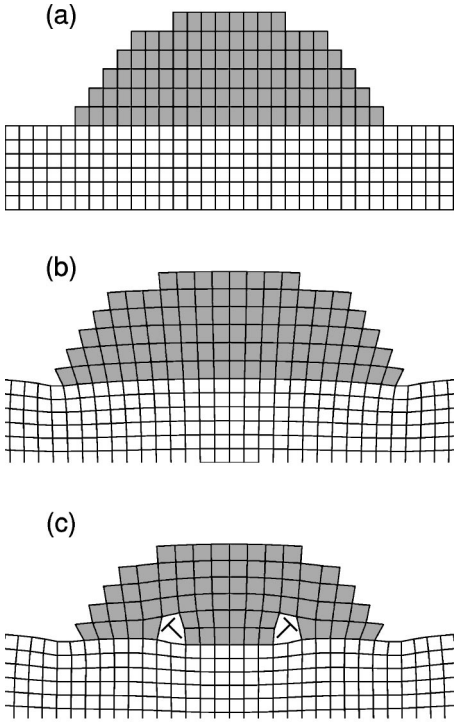

FIG. 4. Deformation and strain relief in equilibrium islands. (a) Unrelaxed configuration for a large island ($V=10$) with uniform 25% compressive misfit, (b) deformations due to strain relaxation in the coherent island, and (c) deformations in island with mixed-type dislocations at ''optimal'' locations (see text).

To illustrate the deformations induced by these misfit dislocations, we introduce a dislocation at each of the energy minima of Figs. 2(h,j). To plot the distortions on the simple square lattice of Fig. 4 we choose dislocations with Burgers vectors $\boldsymbol{b}=b_0(+1,0,-1)$ and $\boldsymbol{b}=b_0(+1,0,+1)$ as the mixed-type square-lattice analog of the misfit dislocations $\boldsymbol{b}=(+1/2,\pm 1/2,-1/\sqrt{2})$ and $\boldsymbol{b}=(+1/2,\pm 1/2,+1/\sqrt{2})$ in the fcc system, and take b_0 as the lattice spacing of the grid. The distortions due to each dislocation are approximated using the displacements generated by a dislocation in an infinite body[43] with components $\boldsymbol{b}=(b_x,0,b_z)$:

$$u_x=\frac{b_x}{2\pi}\left[\tan^{-1}(-z'/x')-\frac{x'z'}{2(1-\nu)r^2}\right]-\frac{b_z}{2\pi}\left[\frac{(1-2\nu)}{4(1-\nu)}\ln r^2+\frac{(z')^2-(x')^2}{4(1-\nu)r^2}\right], \tag{8}$$

$$u_z=\frac{b_x}{2\pi}\left[\frac{(1-2\nu)}{4(1-\nu)}\ln r^2+\frac{(x')^2-(z')^2}{4(1-\nu)r^2}\right]+\frac{b_z}{2\pi}\left[\tan^{-1}(x'/z')+\frac{x'z'}{2(1-\nu)r^2}\right], \tag{9}$$

where x' and z' is the point position relative to the dislocation and $r^2=(x')^2+(z')^2$. The resulting distortions caused by the two dislocations when placed in the island are shown in Fig. 4(c). The placement of these dislocations on opposite sides of the island results in optimal strain relief through the relaxation in directions tangential to the island surface (i.e,. a relaxation of the ''hoop strain'' along the island surface), as well as an unbuckling of the film/substrate interface.

The calculations presented here for two-dimensional islands demonstrate that misfit dislocations have minimum-energy positions that depend on the orientation of the Burgers vector. This suggests that misfit dislocations in a two-dimensional island ridge will segregate by type, as in Fig. 4(c). The segregation mechanism for dislocations also applies for fully three-dimensional islands, but the energetics of introducing dislocation lines need to be modified by the three dimensionality of the stress field as well as the fact that the length of the dislocation line varies with its position in the island cross section.

V. SUMMARY

We have presented detailed results for the stresses that accompany isolated equilibrium Stranski-Krastanow islands in two dimensions (ridges). These island shapes and stresses are determined by numerical solution of the coupled stress and free boundary problem. These results show that as the island size increases the overall trend is for relaxation of the misfit strain over most of the volume of the island; however, relaxation is not complete. In addition to the focusing of the stress concentration near the island edge, there are also regions of stress adjacent to the film/substrate interface which correspond to partial relaxation of the stress in the film and compliance by the substrate to accommodate the misfit. The short-range lateral decay of the stresses away from the islands is a factor in the changes in island shapes as neighboring islands impinge upon one another.

We have also used the stresses in a first-order calculation of the energy of introducing a dislocation anywhere in the system. These calculations demonstrate that the pure edge dislocation is the most energetically favorable with an energy minimum lying directly underneath the center of the island. On the other hand, 60° misfit dislocations have an energy minimum that lies under one side of the island or the other, depending on the orientation of the Burgers vector. This orientation dependence of the position of the energy minimum suggests that dislocations are segregated in the island by orientation, and we confirm that the predicted segregation is consistent with kinetic and glide constraints of dislocation introduction in the limits of small and large driving forces. Physically, this segregation can be explained in terms of distributing the dislocations most efficiently to relieve the misfit and shear stress in the island.

ACKNOWLEDGMENTS

This research was supported by NSF Grants Nos. DMS-9622930 and DMS-0072532 (B.J.S).

[1] P. M. Petroff and G. Medeiros-Ribeiro, MRS Bull. **21** (4), 50 (1996).
[2] B. G. Levi, Phys. Today **49** (5), 22 (1996).
[3] R. J. Asaro and W. A. Tiller, Metall. Trans. **3**, 1789 (1972).
[4] M. A. Grinfel'd, Dokl. Akad. Nauk (SSSR) **290**, 1358 (1986) [Sov. Phys. Dokl. **31**, 831 (1986).
[5] R. Bruinsma and A. Zangwill, Europhys. Lett. **4**, 729 (1987).
[6] D. J. Srolovitz, Acta Metall. **37**, 621 (1989).
[7] H. Gao, in *Modern Theory of Anisotropic Elasticity and Applications*, edited by J. J. Wu, T. C. T. Ting, and D. M. Barnett (SIAM, Philadelphia, 1991), pp. 139–150.
[8] B. J. Spencer, P. W. Voorhees, and S. H. Davis, Phys. Rev. Lett. **67**, 3696 (1991).
[9] L. B. Freund and F. Jonsdottir, J. Mech. Phys. Solids **41**, 1245 (1993).
[10] J. Grilhe, Acta Metall. Mater. **41**, 909 (1993).
[11] M. A. Grinfeld, J. Nonlinear Sci. **3**, 35 (1993).
[12] N. Junqua and J. Grilhé, J. Phys. III **3**, 1589 (1993).
[13] B. J. Spencer, P. W. Voorhees, and S. H. Davis, J. Appl. Phys. **73**, 4955 (1993).
[14] J. Tersoff and F. K. LeGoues, Phys. Rev. Lett. **72**, 3570 (1994).
[15] J. Tersoff and R. M. Tromp, Phys. Rev. Lett. **70**, 2782 (1990).
[16] D. Vanderbilt and L. K. Wickham, in *Evolution of Thin Film and Surface Microstructures*, edited by C. V. Thompson, J. Y. Tsao, and D. J. Sroloviz, Mater. Res. Soc. Symp. Proc. No. 202 (Materials Research Society, Pittsburgh, 1991), p. 555.
[17] B. G. Orr, D. Kessler, C. W. Snyder, and L. Sander, Europhys. Lett. **19**, 33 (1992).
[18] C. Ratsch and A. Zangwill, Surf. Sci. **293**, 123 (1993).
[19] H. Gao, J. Mech. Phys. Solids **42**, 741 (1994).
[20] M. Albrecht, S. Christiansen, J. Michler, W. Dorsch, H. P. Strunk, P. O. Hansson, and E. Bauser, Appl. Phys. Lett. **67**, 1232 (1995).
[21] C. H. Chiu and H. Gao, in *Thin Films: Stresses and Mechanical Properties V*, edited by S. P. Baker, P. Børgesen, P. H. Townsend, C. A. Ross, and C. A. Volkert, Mater. Res. Soc. Symp. Proc. No. 356 (Materials Research Society, Pittsburgh, 1995), p. 33.
[22] L. J. Gray, M. F. Chisholm, and T. Kaplan, Appl. Phys. Lett. **66**, 1924 (1995).
[23] D. J. Eaglesham and R. Hull, Mater. Sci. Eng., B **30**, 197 (1995).
[24] A. G. Cullis, MRS Bull. **21** (4), 21 (1996).
[25] L. B. Freund, H. T. Johnson, and R. V. Kukta, in *Evolution of Epitaxial Structure and Morphology*, edited by A. Zangwill, D. Jesson, D. Chambliss, and R. Clarke, Mater. Res. Soc. Symp. Proc. No. 399 (Materials Research Society, Pittsburgh, 1996), p. 359.
[26] B. J. Spencer and J. Tersoff, in *Evolution of Epitaxial Structures and Morphology* (Ref. 25), p. 283.
[27] A. L. Barabási, Appl. Phys. Lett. **70**, 2565 (1997).
[28] I. Daruka and A. L. Barabási, Phys. Rev. Lett. **79**, 3708 (1997).
[29] H. T. Johnson and L. B. Freund, J. Appl. Phys. **81**, 6081 (1997).

[30] R. V. Kukta and L. B. Freund, J. Mech. Phys. Solids **45**, 1835 (1997).
[31] B. J. Spencer and J. Tersoff, Phys. Rev. Lett. **79**, 4858 (1997).
[32] I. Daruka and A. L. Barabasi, Appl. Phys. Lett. **72**, 2102 (1998).
[33] B. J. Spencer and J. Tersoff, in *Mathematics of Multiscale Materials*, edited by K. M. Golden, G. R. Grimmett, R. D. James, G. W. Milton, and P. N. Sen (Springer-Verlag, New York, 1998), pp. 255–269.
[34] C. Duport, C. Priester, and J. Villain, in *Morphological Organization in Epitaxial Growth and Removal*, edited by Z. Zhang and M. Lagally (World Scientific, Singapore, 1997).
[35] J. K. Lee, in *Dynamics of Crystal Surfaces and Interfaces*, edited by P. M. Duxbury and T. Pence (Plenum, New York, 1997), pp. 125–134.
[36] B. J. Spencer and J. Tersoff, Appl. Phys. Lett. **77**, 2533 (2000).
[37] B. J. Spencer, Phys. Rev. B **59**, 2011 (1999).
[38] B. J. Spencer and D. I. Meiron, Acta Metall. Mater. **42**, 3629 (1994).
[39] M. L. Williams, J. Appl. Mech. **19**, 526 (1952).
[40] J. A. Floro, G. A. Lucadamo, E. Chason, L. B. Freund, M. Sinclair, R. D. Tweston, and R. Q. Hwang, Phys. Rev. Lett. **80**, 4717 (1998).
[41] J. Y. Tsao, *Materials Fundamentals of Molecular Beam Epitaxy* (Academic Press, New York, 1993).
[42] F. K. LeGoues, M. C. Reuter, J. Tersoff, M. Hammar, and R. M. Tromp, Phys. Rev. Lett. **73**, 300 (1994).
[43] J. P. Hirth and J. Lothe, *Theory of Dislocations* (Wiley, New York, 1982).
[44] J. E. Ayers and L. J. Schowalter, Phys. Rev. Lett. **72**, 4055 (1994).
[45] F. K. LeGoues, P. M. Mooney, and J. Tersoff, Phys. Rev. Lett. **71**, 396 (1993); **72**, 4056 (1994).